

Explaining random forest predictions through diverse rules

Klest Dedja^{1,2,*}, Felipe Kenji Nakano^{1,2}, Konstantinos Pliakos³, and Celine Vens^{1,2}

¹Department of Primary Care, Kortrijk, KU Leuven

²Itec, imec research group, Kortrijk, KU Leuven

³Department of Management, Strategy, and Innovation, KU Leuven

*corresponding author, emails are: {firstname.lastname}@kuleuven.be

Abstract

Tree-ensemble algorithms, such as random forest, are effective machine learning methods popular for their flexibility, high performance, and robustness to overfitting. However, since multiple learners are combined, they are not as interpretable as a single decision tree. In this work we propose a methodology, called Local Tree eXtractor (LTreeX) which is able to explain the forest prediction for a given test instance with a few diverse rules. Starting from the decision trees generated by a random forest, our method 1) pre-selects a subset of them, 2) creates a vector representation, and 3) eventually clusters such a representation. Each cluster prototype results in a rule that explains the test instance prediction. We test the effectiveness of LTreeX on 71 real-world datasets and we demonstrate the validity of our approach for binary classification, regression, multi-label classification and time-to-event tasks. In all set-ups, we show that our extracted surrogate model manages to approximate the performance of the corresponding ensemble model, while selecting only few trees from the whole forest. We also show that our proposed approach substantially outperforms other explainable methods in terms of predictive performance.

Keywords— Explainable AI, Interpretable ML, Random Forest, Random Survival Forest, Multi-label classification

1 Introduction

Machine Learning (ML) models are nowadays employed in various domains with excellent performance. When the performance is key to having a competitive advantage, ML models are widespread even when the algorithmic procedure is too complicated to be understood by humans (so called “black box” algorithms). However, in fields where the stakes for a single decision are

high (healthcare, banking, etc.) [1] there is still scepticism in adopting such models. Professionals are accountable for any costly mistake, and in such cases they want to fully understand and trust the outcomes of a ML model. An important element that leads them to trust ML models and therefore transition towards them is to achieve more explainability in ML [2]. In recent years, the ML community has therefore been developing tools that help ML practitioners and

end-users understand the predictions of black box models, thus leading to the booming of the field of Explainable AI (X-AI). The approaches are plenty and the field has not reached convergence neither from the methodological point of view, nor, as Molnar et al. observe [3], in the definition of interpretability.

However, all these approaches can be split into a few categories. The most common distinction groups these methods into *global* and *local* explanations.

Global explanations aim at explaining the model as a whole. Partial Dependency Plots [4], for instance, and its later extensions (e.g. [5]) assist in visualising the average partial relationship between the model prediction and a set of features, with the result being a plot of such functional relationship.

Local explanations, on the other hand, aim at explaining the reason why a certain prediction was made for a given instance. An example of this is LIME [6], a toolbox that linearly approximates a model around a neighbourhood of the predicted instance that needs to be explained. Another successful local approach is SHAP [7], an explainability toolbox that outputs the contribution that every feature value has towards a given model prediction.

Many of the proposed explainability techniques are model agnostic, meaning that they do not take into account the specific characteristics of the model they are explaining. Next, they often result in a single explanation, whereas in many cases multiple viable explanations can be attached to a certain prediction. Moreover, to our knowledge, most explainability methods are designed for and have been evaluated on standard machine learning tasks, such as binary classification and regression.

In this study, we propose a novel method

that summarises a random forest (RF) [8] into a few trees, which are members of the forest. This way, our so-called surrogate model uses information directly extracted from the original model. At the same time, it provides different insights by selecting dissimilar trees. Our proposed method, called LTreeX, follows a local approach and, hence, extracts different decision trees (or equivalently, decision paths or rules) for different instances. The choice to specifically explain RF predictions is driven by the fact that RF has a great predictive performance and is computationally more efficient as well as easier to train than other highly performing methods, such as deep neural networks. Moreover, RF has been extended to a wide range of learning tasks, including binary classification, multi-label classification, regression and time-to-event prediction. Our method is designed in such a way that it is independent of the learning task at hand, and consequently, it is capable of handling all these scenarios.

LTreeX is built on top of a trained random forest and consists of four main steps. First, a subset of trees is selected based on how close their prediction is with respect to the original ensemble. Next, we build a vector representation of such trees by extracting information from the tree structure. Dimensionality reduction of such representations is then performed as a third step and lastly, we apply clustering on this tree representation, extracting this way only a few prototype rules. These final rules are then presented to the end user as an explanation for the forest prediction. By keeping the number of prototype rules low, we provide a few diverse explanations, which can be inspected by the user.

Preliminary results of this work were presented in an earlier workshop [9] and were restricted to binary and time-to-event predictions.

Here, we extend this work to regression and multi-label classification as well as improving the implementation of the algorithm. Furthermore, we also provide a thorough experimental evaluation of our approach, and an ablation study which validates the steps in our method. Overall, our contributions to the field of X-AI can be summarised as follows:

- We propose a local approach for explaining RFs by extracting a few meaningful trees (or paths) from a trained RF. The simplified model is able to mimic the prediction of the RF and is able to provide the user with a limited number of different explanations for the prediction. Furthermore, such a model contains a subset of the trees of the original ensemble predictor and therefore reveals parts of the original black-box model.
- We evaluate our local explainer in four different scenarios: binary classification, regression, multi-label classification and time-to-event prediction, the latter two being seldom explored in existing explainability toolboxes.
- We report the achieved predictive performance of our surrogate model, together with the average dissimilarity of the extracted trees, using 71 real world datasets. The obtained results are compared to the original RF, single decision trees (DTs), two baseline methods to obtain a small number of trees from a RF, a regression method and a recent related method from the literature.
- We make our methodology available to the ML community and the public by providing a Python implementation through

GitHub (link will be provided upon acceptance), compatible with scikit-learn and scikit-survival.

The remainder of the manuscript is organised as follows: Section 2 positions our work within the frame of local explainers based on RF, and underlines the differences with the existing literature; Section 3 provides the background information for the method section, where our model is introduced (Section 4). These are followed by Section 5, dedicated to the experimental set-up and Section 6, where the performance and dissimilarity results are reported together with the outcomes of the ablation study. We discuss such results and provide two examples of explanations by LTreeX in the second part of Section 6. Finally, we draw our conclusions in the last part of the manuscript (Section 7).

2 Related work

As explained in the introduction, there are a few dimensions along which we can classify explainability methods. In addition to the distinction between local and global approaches, we can categorize them according to whether they depend on the underlying model, resulting in model agnostic (e.g. the methods mentioned in the introduction) and model specific ones. Model specific explainers can make use of inherent characteristics or knowledge from the model that they aim to explain, and usually rely on popular ML algorithms with excellent performance such as RFs or deep neural networks. Our proposed approach LTreeX falls into this category as it uses the trees (or, according to the configuration, the rules) generated by the underlying trained random forest to explain a prediction. Here, we discuss other model specific approaches that use

RFs as the underlying black-box model.

The earliest example of such model specific methods is [10]. Their work proposed a procedure for analysing a RF, and concepts such as *tree-metric*, a distance metric defined on the space of tree learners, are also introduced. Trees are then represented in a two-dimensional space by using Multi Dimensional Scaling [11] on the tree-distance matrix. The authors then perform a qualitative study and mention the possibility of clustering the resulting tree representations.

Later work by [12] made use of a tree-distance metric intuition to project tree paths via t-SNE [13], and made also use of visual analytics to improve interpretability. These visuals include a “feature view” that shows the relationship between a selected feature and a prediction (similarly to a Partial Dependency plot) as well as a control panel that just lets the user see the decision paths that lead to the prediction of a group of instances. Unlike LTreeX, there is no rule extraction or forest approximation mechanism and none of the original learners are shown to the end user.

A different approach came from [14], in this case the authors adopted a model-agnostic approach, where a model is used as an oracle that can be queried, and a single tree is grown in order to best fit such an oracle. The growth of such tree follows a novel best split rule where synthetic samples are generated until the best split is statistically identified. Unlike LTreeX, a single decision tree is grown in this case and furthermore, the growth of such tree is inherently different from the ones that are generated following Breiman’s procedure, or in general the learning process of the original tree-ensemble model.

Other relevant approaches include [15], where the authors presented a method for computing how a feature within a value range influ-

ences the final prediction of a model, while an optimisation-based approach that exploits the bijective relationship between a tree leaf and a subspace of the input space is proposed by [16].

Finally, a recent work by [17] was built upon the aforementioned [10], suggesting a range of tree-distance similarity measures (tree-metrics) and performing clustering on such tree representations. The authors extracted a few trees out of a random forest and illustrate the validity of their methodology using only a single empirical dataset. However, they do not investigate the prediction performance of the obtained surrogate model, nor does their tree selection depend on the sample to be explained, making it a global approach instead.

3 Background

Random forest (RF) is a computationally efficient ML method that delivers excellent predictive performance, and since its appearance, RFs have been extremely successful in performing classification and regression tasks. Moreover, RFs have been extended to a variety of other learning tasks, including multi-label classification and survival analysis. Most of the extensions and adaptations that have been proposed over the years are associated with the node splitting mechanism as well as the prototype function (i.e., the function that provides predictions in the leaves), while less modifications have been proposed for other RF characteristics, such as the bootstrapping.

A common splitting criterion for RFs in binary classification is the Gini impurity index, whereas a common prototype function returns the most frequent class label among training instances falling in the leaf. For regression tasks,

the splitting rule that maximally reduces intra-node variance in the target values is usually chosen, and the average target value is returned as prediction.

In multi-label classification, a single instance may belong to multiple classes and, hence, the task is to predict the correct subset of class labels for each instance. Multi-label classification has many applications, including text classification, image annotation, protein function prediction, etc. Several machine learning methods have been adapted to multi-label classification, including random forests [18, 19]. In order to take into account the multiple labels, the splitting criterion is adapted by maximising either the average impurity reduction [19] or average variance reduction [20], across all the (binary) labels. These criteria implicitly take into account label dependence and are often preferred to methods that train output labels independently [18]. In both cases, the leaves return a vector, where each component represents the proportion of instances annotated with the corresponding label.

Survival analysis is a branch of statistics that has only recently been explored in the machine learning community [21]. The goal of such analysis is to predict the time until an event occurs (hence, this task is also known as time-to-event prediction). Applications include clinical studies, where the outcome of interest is the time until a patient dies, suffers from complications, is discharged from hospital, etc. A key challenge in this field is the so called *censoring* effect, that is when the exact time of the event is not observed, resulting in partial information. For instance, in the case of right censoring, which is the type of censoring included in our study, the recorded event time is an underestimate of the true time. This may for instance

occur when a patient drops out from the study or has not reached the outcome event before the study end. Decision trees and random forests (as well as other machine learning methods) have been adapted to survival data, they are called (Decision) Survival Trees [22, 23] and Random Survival Forests (RSF) [24], respectively. The main splitting criterion being used is the *logrank* score [25], a criterion that guarantees good generalisation for censored time-to-event data [24]. This criterion aims at splitting the population in maximally different subgroups with maximally different hazard functions. At each leaf node, a Kaplan-Meier [26] estimate of the survival function for the population that falls in that node is built.

4 Proposed Method

Let \mathcal{T} be a random forest. We first extract τ trees $\mathcal{T}_i \in \mathcal{T}$ that generate the most similar predictions to the whole ensemble model \mathcal{T} . More specifically, given a sample x and its ensemble prediction $\hat{y} = \mathcal{T}(x)$, we select the τ trees whose predictions are closest in value to \hat{y} . Next, we represent each of the selected trees \mathcal{T}_i as a vector, this vector can be a function of the tree structure, or also depend on the sample whose prediction we want to explain. Two approaches arise from this, namely:

- A full *tree-based* vectorisation: here we record the splitting covariates used in *every* internal split of the tree; assuming that there are p input features, we obtain the number of splitting occurrences g_1, g_2, \dots, g_p , and the tree representation becomes:

$$\mathcal{T}_i(x) \rightarrow \vec{g}_i = [g_{i1}, g_{i2}, \dots, g_{ip}]. \quad (1)$$

This representation was proposed by [17], where a variety of possibilities was presented, and it consists of an adaptation of the approach from [27], that considered a binary representation. We prefer the former representation over a binary one for its ability to take into account multiple splits on the same feature.

- A *path-based* vector representation where the sample of interest x traverses the tree and the input covariate used to perform each split is recorded. When the sample reaches a leaf, the process stops and the representation $[f_1, f_2, \dots, f_p]$ consists of the number of times each feature is selected to perform a split along the path. The path-based representation of the tree is therefore:

$$\mathcal{T}_i(x) \rightarrow \vec{f}_i = [f_{i1}, f_{i2}, \dots, f_{ip}], \quad (2)$$

which can be seen as a local variation of the previous approach.

Notice that, unlike the tree-based approach, the path-based vector representation of \mathcal{T}_i depends on the sample of interest x , and, thus, is more tailored towards the task at hand. On the other hand, the tree-based vectorisation has the computational advantage of only having to be computed once for every tree in the forest.

Next, we project such vector representations to a lower dimensional space using Principal Component Analysis (PCA) [28]. The idea is to remove the noise from the representation, to improve computational efficiency for later steps, and to enable a better visualisation of the subsequent clustering.

In order to obtain a diverse set of explanations, as the next step, we perform clustering

on the low-dimensional tree representation using a standard clustering method, such as K-Means [29]. An example of the clustering step is shown in Figure 1. By means of this, the trees are grouped into K clusters and for each cluster k we find the tree \mathcal{T}_{i_k} closest to the cluster centre, and we pick it as representative for explaining the outcome of the model. We call such trees *final candidates*. Each final candidate produces one rule, composed by the conjunction of tests along the decision path that explains the instance under consideration. Given K clusters, the corresponding final candidates \mathcal{T}_{i_k} , and an instance x , the final surrogate model prediction \bar{y} is built as follows:

$$\bar{y} = \sum_{k=1}^K w_k \mathcal{T}_{i_k}(x) \quad (3)$$

where w_k represents the weight given to the cluster k . We define w_k as the proportion of trees that are part of the cluster. It follows that $\sum w_k = 1$, and that the surrogate model is a weighted average of the chosen trees.

Our method requires three hyperparameters: the number of trees τ to keep in the pre-selection phase, the number of output components d for PCA, and the number of clusters K . The optimal values can be tuned for each test instance separately, by calculating the *faithfulness* of the surrogate model to the original ensemble. This measure is an indicator of how closely the original ensemble prediction is being imitated by our surrogate model. Given an instance x , the prediction made by the original R(S)F \hat{y} and the new surrogate prediction \bar{y} , we define and compute faithfulness $\mathcal{F}(x)$ as:

$$\mathcal{F}(x) = 1 - \|\hat{y} - \bar{y}\|_2. \quad (4)$$

Depending on the set-up, \hat{y} and \bar{y} are either

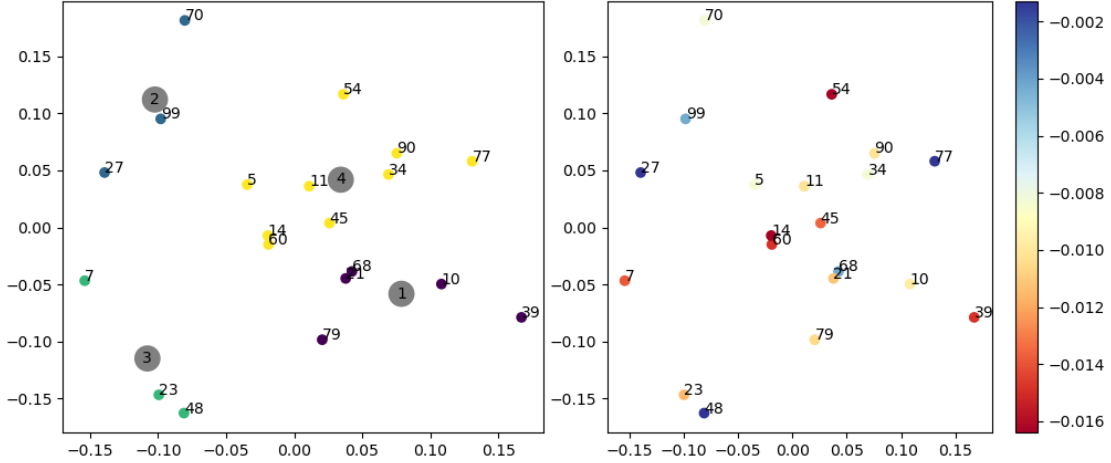


Figure 1: Left side: Example of the clustering step following tree pre-selection, vectorisation and PCA for the “blood” dataset (binary task, see Section 6.1 for details) and a random test instance x . The centroids of the K-Means algorithm (with $K=4$) are shown in grey, and the cluster membership is depicted in color. In this case, trees 10, 99, 23 and 11 are selected as final candidates. Right side: Difference between the individual trees’ predictions and the RF prediction for x . For the final candidates, this difference is measured using the faithfulness measure.

scalars for predicted probabilities (binary classification), estimated scalar values (regression), vectors of predicted class probabilities (multi-label classification), or scalar predicted risk scores (survival analysis). Note that $\mathcal{F}(x) = 1$ for a given instance x indicates perfect faithfulness of LTreeX to the original model. As a result, the hyper-parameter combination $(\bar{K}, \bar{d}, \bar{\tau})$ that maximises \mathcal{F} can be chosen.

An important advantage of our method is that it does not require an external validation set to tune these hyperparameters; the proposed method looks instead at the *predicted* labels from the underlying RF model which at this stage serves as an oracle. The hyperparameters that, for a given test instance, yield the prediction closest to the underlying RF prediction are the

ones selected. By doing so, we increase the faithfulness of the model to the underlying black box, and we concurrently allow a more efficient use of data, since a greater fraction of it can be used to train the underlying model instead of being left aside for the sake of hyperparameter tuning.

Alternatively, the parameter values can be determined by the user. In the latter case, end-users have the option to choose, for example, the number of clusters and thus, explore the trade-off between having a simple (single) explanation against obtaining multiple (different) explanations for a given example.

5 Experiments

We test our tree and path-based approaches across multiple datasets and tasks so that the validity of our approach can be thoroughly investigated. The datasets, unless otherwise specified, are selected from publicly available sources and repositories such as UCI¹ and MULAN² or downloaded from sklearn’s library³. The final list includes as many as 71 datasets, and they consist of:

- 24 binary classification datasets,
- 15 survival analysis datasets (predict time-to-event),
- 19 regression datasets,
- 13 multi-label classification datasets.

5.1 Data and pre-processing

A detailed overview of the datasets of our study follows in the upcoming tables. Starting with the binary classification set-up in Table 1, we show the datasets, together with their size and the prevalence of the positive class.

Similarly, for the time-to-event case, a summary is provided in Table 2, and the censoring rate is reported. We included both small and relatively large datasets (such as the case of the ALS dataset), as well as both low- and high-dimensional datasets, with DLBCL (Diffuse large B-cell lymphomas) being an example of the latter. Some of these datasets contain missing values, which we handle as follows. We drop any observation (row) and covariate (column) with

¹<https://archive.ics.uci.edu/ml/datasets.php>

²<http://mulan.sourceforge.net/datasets-mlc.html>

³<https://scikit-learn.org/stable/modules/classes.html>

Table 1: Overview of the datasets for binary classification tasks. The number of samples n and covariates p is indicated in brackets, class distribution is reported in the last column.

| | data size (n, p) | % positive class |
|------------------------------|-------------------------|---------------------|
| blood | (748 , 4) | 24 |
| B.C. ¹ diagnostic | (569, 30) | 37 |
| B.C. ¹ | (699, 10) | 34 |
| B.C. ¹ prognostic | (198, 33) | 24 |
| B.C. ¹ coimba | (116, 9) | 55 |
| Colon. Green ² | (98, 62) | 68 |
| Colon. Hinsel. ² | (97, 62) | 85 |
| Colon. Schiller ² | (92, 62) | 73 |
| divorce | (170, 54) | 49 |
| Flowmeters | (87, 36) | 60 |
| haberman | (306, 3) | 26 |
| hcc-survival | (165, 49) | 62 |
| ionosphere | (351, 34) | 36 |
| LSVT voice | (126, 310) | 67 |
| mamographic | (961, 5) | 46 |
| musk | (476, 166) | 43 |
| parkinson | (756, 753) | 75 |
| risk factors | (858, 35) | 6 |
| simulation crashes | (540, 18) | 91 |
| sonar | (208, 60) | 53 |
| SPECT | (267, 22) | 79 |
| SPECTF | (267, 44) | 79 |
| vertebral column | (310, 6) | 68 |
| wholesale | (440, 7) | 32 |

more than 30% missing entries and we subsequently impute the missing values of the remaining samples through MICE [30, 31]. This procedure was applied to the ALS dataset ⁴, NHANES

⁴obtained from the Pooled Resource Open-Access ALS

I⁵, Breast Cancer survival and FLChain data.

Table 2: Overview of the time-to-event datasets with right-censored observations, the censoring rate is reported on the rightmost column.

| | data size (n, p) | censoring rate (%) |
|--|-------------------------|-----------------------|
| addicts | (238, 3) | 37 |
| ALS | (5324, 76) | 67 |
| B.C. ¹ survival | (198, 80) | 74 |
| DBCD | (295, 4919) | 73 |
| DLBCL | (240, 7399) | 43 |
| echocardiogram | (130, 9) | 32 |
| FLChain | (7874, 8) | 72 |
| gbsg2 | (686, 8) | 56 |
| lung | (228, 8) | 28 |
| NHANES I | (9931, 18) | 65 |
| primary biliary cirrhosis | (403, 19) | 56 |
| rotterdam (excl. recurr ²) | (2982, 11) | 57 |
| rotterdam (incl. recurr ²) | (2982, 12) | 57 |
| veteran | (137, 9) | 7 |
| whas500 | (500, 14) | 57 |

For the regression tasks (see Table 3), imputation with MICE was needed for a few instances in the datasets indicated by the table. The target covariate for PRSA data spans across different orders of magnitude and is therefore log transformed; furthermore, categorical data in the student final maths dataset are one-hot encoded. To conclude the data processing step, we normalise the target values y to the $[0, 1]$ interval.

Finally, multi-label classification data is con-

Clinical Trials (PRO-ACT) Database. The data available in the PRO-ACT Database have been volunteered by PRO-ACT Consortium members.

⁵www.cdc.gov/nchs/nhanes/about_nhanes.html

Table 3: Regression task datasets

| | data size (n, p) |
|-----------------------------------|-------------------------|
| airfoil | (1503, 5) |
| Ames Housing | (2915, 283) |
| auto mpg ¹ | (398, 7) |
| bike sharing | (731, 12) |
| boston housing | (506, 14) |
| california housing | (20640, 8) |
| car imports ¹ | (201, 63) |
| Computer hardware | (209, 6) |
| concrete compress | (1030, 8) |
| concrete slump | (103, 9) |
| ENB2012 cooling | (768, 8) |
| ENB2012 heating | (768, 8) |
| forest fires | (517, 12) |
| PRSA data | (41757, 13) |
| slump dataset | (103, 9) |
| students final maths ² | (395, 43) |
| wine quality all | (6497, 12) |
| wine quality red | (1599, 11) |
| wine quality white | (4898, 11) |

sidered. We include datasets of varying size both in the number of samples, in the number of input covariates, as well as in the number of output targets denoted as “labels”. The necessary cleaning steps were performed similarly to the previously described scenarios while no MICE imputation was necessary. More details on the datasets are shown in Table 4.

5.2 Performance and dissimilarity

The predictive performance of our surrogate models is computed by means of commonly used measures in each of the four tasks. More specifically, we evaluate the Area Under the Receiver

Table 4: Datasets that include a multi-label classification

| | data size (n, p) | number of labels |
|---------------|-------------------------|---------------------|
| birds | (645, 260) | 19 |
| CAL500 | (502, 68) | 174 |
| emotions | (593, 72) | 6 |
| enron | (1702, 1001) | 53 |
| flags | (193, 19) | 7 |
| genbase | (662, 1185) | 27 |
| langlog | (1460, 1004) | 75 |
| medical | (978, 1449) | 45 |
| ng20 | (4379, 1006) | 20 |
| scene | (2407, 294) | 6 |
| slashdot | (3782, 1079) | 22 |
| stackex chess | (1675, 585) | 227 |
| yeast | (2417, 103) | 14 |

Operator Characteristics (AUROC) for binary classification, the weighted average AUROC in multi-label classification (averaged over each label with weight proportional to the number of true instances of the label), mean absolute error (MAE) for regression tasks, and Concordance Index (C-index) for the survival analysis data.

In addition to the predictive performances, we also consider the dissimilarity of the final explanations, as we want to avoid redundant explanations. For this purpose, we define a distance on the tree-representation space. We use a generalised version of the Jaccard similarity index by [17], where the ratio between the element-wise minimum and maximum of two vectors is taken. Namely, given two tree representations \vec{w}_i and \vec{w}_j , we compute:

$$\mathcal{J}(\vec{w}_i, \vec{w}_j) = \frac{\sum_{k=1}^p \min(w_{ik}, w_{jk})}{\sum_{k=1}^p \max(w_{ik}, w_{jk})}. \quad (5)$$

To obtain a dissimilarity \mathcal{D}_i relative to sample x_i , we consider $1 - \mathcal{J}$ and compute the average pairwise dissimilarity between all K final candidate trees:

$$\mathcal{D}_i = \frac{1}{K(K-1)} \sum_{\substack{l, j \in \{i_1, \dots, i_K\} \\ l \neq j}} 1 - \mathcal{J}(u_l, u_j) \quad (6)$$

\mathcal{D}_i is computed for every test sample, and the average \mathcal{D} across all test data is recorded. We compare the resulting value, when relevant, to the competing approaches. We consider both the tree-based (1) as well as the path-based (2) vectorisation approach in our analysis.

5.3 Experimental setup

In all experiments, we trained the original RF with 100 base learners. As stopping criterion, we required that leaves included at least 5 samples, and at least 10 for the survival analysis set-up. No post-pruning techniques were applied.

Both predictive performance and dissimilarity measures are reported after a 5-fold cross validation is performed, and the test sample size for datasets exceeding 500 entries is limited to 100 for computational reasons⁶. In the multi-label classification setting, we drop target labels that do not occur in the training or testing folds, since the weighted AUROC measure would not be defined for those labels.

With regards to hyperparameter tuning for our approach, the following values are tested in a grid search fashion: As explained earlier, these values are optimised for each test sample individually. The rationale behind these grid values aims at serving multiple goals. First of all, the

⁶Note that the algorithmic procedure of tree extraction, including parameter tuning, is performed for every test sample separately.

Table 5: Hyperparameter space, for every instance the combination with the highest achieved faithfulness \mathcal{F} is chosen.

| name | description | values |
|--------|---|---------------|
| τ | number of pre-selected trees | {10, 20, 50} |
| d | number of dimensions after projection | {2, All} |
| K | number of clusters and final candidates | {1, 2, 3, 4 } |

selected values for τ force the method to select trees that are locally close to the ensemble prediction, with at most 50 trees out of the original 100 making it to the pre-selection phase. Further decreasing the values of τ would, on the other side, hinder the clustering and final-candidate extraction step. Secondly, as for the possible values of the representation dimension d , the value $d = 2$ guarantees that the users can easily visualise the pre-selected trees, while a value of $d = \text{All}$ excludes any dimensionality reduction and retains the most information. In this case the user can still visualise a two-dimensional projection of the tree representation if needed, but the clustering would be performed in the original high-dimensional space. Finally, the values for K are chosen so that at most 4 final candidates are selected, keeping the model fairly explainable.

5.4 Competing methods

The proposed algorithm is compared, in both its tree-based and path-based form, against several competing methods.

The first family of models that we compare LTreeX to, includes ensemble learners built upon a *comparable* number of learners. For this pur-

pose we constructed two approaches, namely a so called “Small R(S)F” as well as a “Best Trees” baseline.

The Small R(S)F method consists of training a Random (Survival) Forest with K base tree learners. For each test sample, the value of K is chosen to be the same as the one used by LTreeX⁷. By doing so, we guarantee that the same number of trees is used by the two methods under comparison. This method serves the purpose of comparing our LTreeX against a baseline that has the same number of tree-learners, generated by the intrinsic randomness of the RF algorithm.

The Best Trees method also consists of a combination of a few trees, selected from the R(S)F. Best Trees first computes out-of-bag (OOB) error for every tree after the training phase, and the best K trees are selected as a final surrogate explanation of the R(S)F. K is again set to the same value as the number of final candidates extracted by LTreeX⁸. Choosing OOB as an indication of tree performance has the advantage of not needing any held-out validation sample, making the comparison with the LTreeX and the Small R(S)F methods fair and straightforward.

A comparison of the dissimilarity measure against Small R(S)F and Best Trees is also useful, as it allows to compare the dissimilarity achieved with LTreeX against the one enforced by the randomness of the RF algorithm on one side, and the one enforced by picking trees according to OOB error on the other. Such dissimilarity is not defined when $K = 1$ (cfr. Equa-

⁷For reporting predictive performance, in the interest of space, K is set as in the path-based LTreeX, although similar values would be observed if the tree-based set-up was used instead.

⁸Again, in its path-based set-up, for reporting predictive performance results.

tion (6)), and therefore such observations are discarded from the comparison. Since the vector representation differs between the tree and the path-based approach, we report such dissimilarities separately. By doing so, we can also investigate whether the choice of the dissimilarity measure has an impact on the results.

Next, we perform a performance comparison with competing methods that are *ante-hoc* explainable, that is, models that are interpretable by design. We consider a single (survival) decision tree as a baseline for all four considered tasks. Furthermore, we include a regularised Logistic Regression with elastic net penalty for binary classification. For the time-to-event scenarios, a regularised Cox-Proportional Hazard (Cox-PH) [32] is deployed with the default `sklearn` settings and in case of failure, the regularisation parameter α is increased. Finally, the role of the simple and *ante-hoc* explainable model for regression tasks is filled by a Ridge regressor.

Furthermore, we compare our method against recent work in literature. For this purpose we select from the related work Section 2 the methods that: 1) have a publicly available source code, and 2) provide a direct way to retrieve the predictions of the surrogate model. The selection narrows down to the C443 [17] method, which is limited to the binary classification set-up. The authors propose a similar approach to our work with their tree extraction algorithm but focus more on giving an overview of the possible approaches rather than optimising the performance of a surrogate model. Furthermore, the C443 methodology aims at global explanations (e.g. by looking at trends and sources of heterogeneity), rather than focusing at an instance-base level. We therefore fill this gap with LTreeX by proposing a local method, and we check whether

a significant performance gain can be achieved. We run the C443 method for the binary classification task (available within the homonym package in R), collect the output trees, and average their prediction for a close comparison. As for the number of clusters to be selected, the authors follow an in-between similarity metric rather than performance and cannot therefore be compared to our approach. For this reason, we run C443 with $K = 3$ clusters, which is a rounded-up estimate of the average number of trees extracted by LTreeX.

Finally, we add the original R(S)F as a baseline, which, together with the single trees, forms two ends of the spectrum in which we operate: on the one hand, we aim for predictive performance close to the R(S)F, while on the other, we aim for an explanation with simplicity close to that of a single tree.

6 Results

In this Section, we report the average performance and dissimilarity achieved by our method across the four different set-up scenarios, both in its tree and path-based vectorisation approach. On the performance side, we compare LTreeX against the competing methods introduced in Section 5.4, especially the more explainable ones. The RF model will be treated as a benchmark for performance. As for the dissimilarity aspect, the average dissimilarity (Equation (6)) of the trees extracted by LTreeX is compared against Small RF and Best Trees, both for the tree as well as the path-based representations. More specifically, for each of the LTreeX approaches, we perform the path or tree-based vectorisation on the competing methods as well, so that a comparison can be made.

Tables with the dataset-specific results are presented for the binary classification data, whereas, to avoid excessive repetition, dataset-specific results from the remaining scenarios are available in the Appendix.

The second step of our analysis consists in testing the statistical significance of the observed differences among methods, and we do so by conducting a post-hoc Friedman-Nemenyi test, setting the significance level to 0.05, as recommended in [33]. Results are visualised with critical difference diagrams, which connect methods that are not statistically significantly different by horizontal line segments [33].

Finally, we present an ablation study; that is, we verify whether the three main steps of the proposed procedure are of added value to the method. The study is repeated for the four tasks evaluated.

6.1 Binary classification

We report the 5-fold cross validated performance for binary classification datasets in Table 6 below. Additionally, the average number of paths extracted by the respective LTreeX approach is shown.

We observe that LTreeX considerably outperforms C443, and its performance is often on par with the original RF. Furthermore, we note a minor difference between the tree based and the path-based approach, and these two methods achieve the highest performance among the interpretable approaches in many cases. The exceptions to this trend are provided by the LR learner which, despite achieving non-remarkable performance on average, appears to be the best model in some datasets (e.g. “blood” and “Colon. Schiller”). This phenomenon might be explained by the intrinsically different (linear)

nature of LR as opposed to the other tree-based models. On the lower end of the spectrum, C443, Small RF, Best trees and DT are not competitive, validating the steps proposed in our method aimed to improve the predictive performance.

By examining the number of paths included in the surrogate model, we notice that a couple of well selected trees are enough to achieve a good level of faithfulness. Moreover, the datasets that generate the lowest number of paths (e.g “B.C. diagnostic”, “B.C. original” and “divorce”) for LTreeX are also the ones for which the models achieve higher performance.

As the next step, we compare the average dissimilarity of the final candidates extracted by LTreeX against the ones generated by Small RF and the ones picked according to the Best Trees approach. The results are shown in Table 7 where both the tree and path-based approach are considered.

We observe that LTreeX achieves the highest dissimilarity in both approaches, for most of the datasets, and it is followed by Small RF and Best Trees in this order. We notice that the latter achieves a much lower dissimilarity in datasets such as “B. C. original” and “divorce”, which are also the ones where a very small number of trees is selected. Finally, we notice that the average dissimilarity values are higher for the path-based approach compared to the tree-based, and this is to be expected due to the sparser nature of the first one, where fewer splits are included while building the representation.

When considering the critical difference diagrams in Figure 2, we can see that the difference between RF and LTreeX is not statistically significant, nor is significant the difference between them and the LR learner. The latter lays approximately in the middle of the spectrum, alternating as we have seen really good AUROC scores

Table 6: Average predictive performance (AUROC) across binary classification datasets. Our proposed methods is shown under the name “LTreeX” in its two approaches: tree and path-based. The highest achieved performance except for RF is shown in bold.

| | RF | LTreeX paths | LTreeX trees | C443 | Best Trees | Small RF | Single DT | Logist. Regress. | average nb. paths |
|------------------|--------|-----------------|-----------------|--------|---------------|---------------|---------------|---------------------|----------------------|
| blood | 0.7080 | 0.7049 | 0.7036 | 0.7228 | 0.6587 | 0.6653 | 0.7048 | 0.7394 | 2.41 |
| B.C. diagnostic | 0.9836 | 0.9876 | 0.9866 | 0.9789 | 0.9435 | 0.9434 | 0.9601 | 0.9645 | 1.33 |
| B.C. original | 1.0000 | 1.0000 | 1.0000 | 0.9999 | 1.0000 | 1.0000 | 1.0000 | 1.0000 | 1.02 |
| B.C. prognostic | 0.5015 | 0.5278 | 0.5170 | 0.5830 | 0.5259 | 0.5315 | 0.5893 | 0.6370 | 2.62 |
| B.C. coimba | 0.7569 | 0.7569 | 0.7392 | 0.6785 | 0.7323 | 0.6977 | 0.7108 | 0.8108 | 2.77 |
| Colon. Green | 0.9333 | 0.8859 | 0.9051 | 0.8167 | 0.7821 | 0.7026 | 0.6962 | 0.6718 | 2.55 |
| Colon. Hinsel. | 0.5917 | 0.5708 | 0.5938 | 0.5438 | 0.6104 | 0.4375 | 0.6146 | 0.4833 | 2.11 |
| Colon. Schiller | 0.6292 | 0.5846 | 0.6046 | 0.5846 | 0.5569 | 0.6215 | 0.5600 | 0.6615 | 2.62 |
| divorce | 0.9941 | 0.9471 | 0.9471 | 0.9360 | 0.9412 | 0.9526 | 0.9349 | 1.0000 | 1.05 |
| Flowmeters | 0.9943 | 0.9971 | 0.9886 | 0.9643 | 0.9471 | 0.8414 | 0.9086 | 0.4771 | 2.18 |
| haberman | 0.6897 | 0.6847 | 0.6815 | 0.6824 | 0.6700 | 0.6267 | 0.6185 | 0.6853 | 2.28 |
| hcc-survival | 0.8331 | 0.8231 | 0.8292 | 0.6335 | 0.6623 | 0.6850 | 0.7162 | 0.4192 | 2.88 |
| ionosphere | 0.9828 | 0.9760 | 0.9805 | 0.9272 | 0.9223 | 0.8562 | 0.9276 | 0.9020 | 1.82 |
| LSVT voice | 0.8824 | 0.8544 | 0.8846 | 0.8353 | 0.7831 | 0.7221 | 0.7699 | 0.6191 | 2.24 |
| mamographic | 0.8523 | 0.8490 | 0.8479 | 0.8469 | 0.8254 | 0.7968 | 0.8355 | 0.8316 | 1.94 |
| musk | 0.9511 | 0.9422 | 0.9404 | 0.8098 | 0.8673 | 0.7765 | 0.7716 | 0.9132 | 2.61 |
| parkinson | 0.9348 | 0.9286 | 0.9285 | 0.7734 | 0.8251 | 0.7792 | 0.7819 | 0.3051 | 1.98 |
| risk factors | 0.9709 | 0.9344 | 0.9348 | 0.7734 | 0.9007 | 0.8580 | 0.9379 | 0.9801 | 1.28 |
| simul. crashes | 0.9284 | 0.9037 | 0.9157 | 0.7264 | 0.8290 | 0.6424 | 0.7594 | 0.9654 | 1.51 |
| sonar | 0.9163 | 0.9199 | 0.9220 | 0.7694 | 0.7763 | 0.7902 | 0.7498 | 0.8455 | 2.60 |
| SPECT | 0.7695 | 0.7530 | 0.7506 | 0.7694 | 0.7450 | 0.7535 | 0.6957 | 0.7870 | 2.16 |
| SPECTF | 0.8203 | 0.7879 | 0.8039 | 0.6879 | 0.6247 | 0.7017 | 0.6485 | 0.7442 | 2.26 |
| vertebral column | 0.9550 | 0.9545 | 0.9550 | 0.8865 | 0.9045 | 0.7933 | 0.8907 | 0.9562 | 1.91 |
| wholesale | 0.9554 | 0.9530 | 0.9528 | 0.9464 | 0.9118 | 0.8349 | 0.9322 | 0.9023 | 1.66 |
| average | 0.8556 | 0.8428 | 0.8464 | 0.7865 | 0.7894 | 0.7504 | 0.7798 | 0.7626 | 2.07 |

Table 7: Average dissimilarity index across binary classification datasets, tree-based and path-based. The dissimilarities achieved by our proposed methods are shown under the name “LTreeX”.

| | LTreeX (trees) | Small RF (trees) | Best Trees (trees) | LTreeX (paths) | Small RF (paths) | Best Trees (paths) |
|------------------|-------------------|---------------------|-----------------------|-------------------|---------------------|-----------------------|
| blood | 0.1805 | 0.1776 | 0.1542 | 0.4741 | 0.4738 | 0.4602 |
| B.C. diagnostic | 0.7533 | 0.7746 | 0.7429 | 0.9010 | 0.8775 | 0.8832 |
| B.C. original | 0.8504 | 0.5943 | 0.0714 | 0.9470 | 0.6861 | 0.0469 |
| B.C. prognostic | 0.7873 | 0.7874 | 0.7840 | 0.9334 | 0.9097 | 0.9023 |
| B.C. coimba | 0.5672 | 0.5699 | 0.4978 | 0.7910 | 0.7416 | 0.7058 |
| Colon. Green | 0.9423 | 0.9347 | 0.8924 | 0.9692 | 0.9559 | 0.9317 |
| Colon. Hinsel. | 0.9510 | 0.9319 | 0.8785 | 0.9760 | 0.9599 | 0.8963 |
| Colon. Schiller | 0.9274 | 0.9224 | 0.9433 | 0.9726 | 0.9453 | 0.9490 |
| divorce | 0.9944 | 0.9722 | 0.3611 | 1.0000 | 0.8790 | 0.7806 |
| Flowmeters | 0.9015 | 0.8748 | 0.8320 | 0.9650 | 0.9112 | 0.8575 |
| haberman | 0.2240 | 0.2146 | 0.1982 | 0.5050 | 0.4639 | 0.4509 |
| hcc-survival | 0.7985 | 0.7964 | 0.7915 | 0.9400 | 0.9097 | 0.9018 |
| ionosphere | 0.7722 | 0.7685 | 0.7581 | 0.9203 | 0.8829 | 0.8645 |
| LSVT voice | 0.9795 | 0.9749 | 0.9673 | 0.9936 | 0.9852 | 0.9851 |
| mamographic | 0.1881 | 0.1779 | 0.1670 | 0.4270 | 0.4259 | 0.4091 |
| musk | 0.9012 | 0.9003 | 0.8911 | 0.9751 | 0.9697 | 0.9660 |
| parkinson | 0.9710 | 0.9664 | 0.9710 | 0.9944 | 0.9917 | 0.9911 |
| risk factors | 0.5780 | 0.5944 | 0.5846 | 0.8404 | 0.8371 | 0.8164 |
| simul. crashes | 0.6162 | 0.6206 | 0.6329 | 0.8028 | 0.8024 | 0.7336 |
| sonar | 0.8718 | 0.8692 | 0.8473 | 0.9632 | 0.9421 | 0.9283 |
| SPECT | 0.4845 | 0.4924 | 0.4563 | 0.7675 | 0.7586 | 0.7196 |
| SPECTF | 0.8154 | 0.8090 | 0.7812 | 0.9426 | 0.9222 | 0.9051 |
| vertebral column | 0.3932 | 0.4018 | 0.3735 | 0.6346 | 0.6375 | 0.5968 |
| wholesale | 0.4187 | 0.4219 | 0.4198 | 0.6720 | 0.6777 | 0.5910 |
| avg. dissim. | 0.7028 | 0.6895 | 0.6249 | 0.8462 | 0.8144 | 0.7614 |

with mediocre performances, and is not statistically better than C443, DT and Best Trees. On the lower end of the performance spectrum we have the two competing methods built ad-hoc together with C443 and DT. We significantly outperform these methods with LTreeX, both with the tree-based and the path-based approach.

The same statistical procedure is run for the dissimilarity metric. The runs are limited to the methods for which tree (or path) dissimilarity is available, namely LTreeX, Small RF and Best Trees. The results are shown in Figure 3 for both tree and path-based dissimilarities.

The post-hoc Nemenyi tests reveal significant

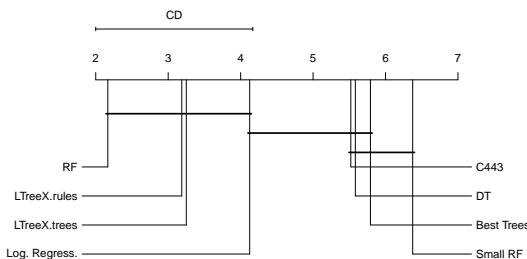


Figure 2: Friedman-Nemenyi test, results regarding performance on binary classification data

differences in dissimilarity across the three methods, with LTreeX achieving the highest. It is also worth noting that the relative performances and the average rankings remain practically unchanged between the two vectorisation approaches.

6.2 Time-to-event prediction

We follow a similar procedure for time-to-event data, providing an overview of the average performance results in Table 8, the reader can find the cross validated average performances of every dataset in Table 12. For this set-up, the regularised Cox-PH model replaces LR in the role of the *ante-hoc* explainable competitor.

The post-hoc analysis with respect to performance (Figure 4) shows a similar trend to the binary case: LTreeX outperforms all competing methods and in this case it even outperforms RF with the tree-based representation set-up. The difference is not significant against Cox-PH, but it is with respect to the other tree-based methods.

The results of the statistical analysis concerning dissimilarity are available in Figure 5. LTreeX again outperforms Small RSF and Best

Survival Trees in terms of dissimilarity among trees, although the difference is not always significant. It is worth noting that, unlike the binary classification scenario, Best Survival Trees achieves higher dissimilarity than Small RSF.

The dataset-specific results for the dissimilarity index are found in Table 13.

6.3 Regression

The analysis of the results for the regression set-up follows the same structure: an overview of the average performance is shown in Table 9, and the details are provided in the Appendix, namely in Table 14. Regularised regression (Ridge) is deployed as a representative for *ante-hoc* explainable methods.

The evaluation procedure involving Friedman’s and Nemenyi’s tests presents results that further affirm the validity of LTreeX in regression tasks. In this case, LTreeX remarkably outperforms RF *both* with the tree-based and the path-based approach, moreover it significantly outperforms all the other competing methods, including regularised Ridge regression. Another difference with respect to the previously analysed set-ups is that the performance of ante-hoc explainable method (Ridge) is considerably worse and falls in the lower end of the spectrum.

The dissimilarity of the extracted trees is validated based on the same procedure as before, and the results are shown in Figure 7. LTreeX again guarantees a high degree of dissimilarity, scoring higher values compared to the competing methods with the same amount of tree learners.



Figure 3: Friedman-Nemenyi test for dissimilarity measure (binary set-up). The full tree-based representation is on the left, the path-based representation on the right.

Table 8: Average achieved Concordance Index (C-index) across datasets. In bold, the best achieved performance excluding the black-box RSF

| RSF | LTreeX paths | LTreeX trees | DST | Best Trees | Small RSF | Cox-PH | avg. nb. of paths |
|--------|--------------|---------------|--------|------------|-----------|--------|-------------------|
| 0.7291 | 0.7286 | 0.7288 | 0.6648 | 0.6859 | 0.6887 | 0.7092 | 2.90 |

Table 9: Average achieved Mean Absolute Error (MAE), multiplied by 100, across datasets. In bold, the best achieved performance excluding the black-box RF

| RF | LTreeX paths | LTreeX trees | avg. nb. of paths | DT | Best Trees | Small RF | Ridge regression |
|--------|--------------|---------------|-------------------|--------|------------|----------|------------------|
| 6.7843 | 6.7286 | 6.7228 | 2.81 | 8.3301 | 8.2433 | 7.8153 | 9.4248 |

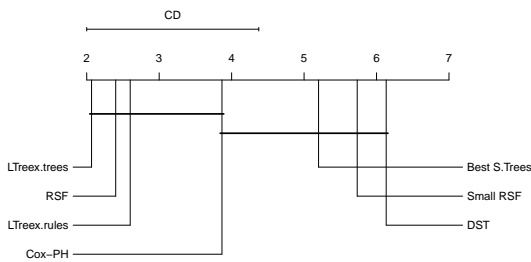


Figure 4: Friedman-Nemenyi test, results regarding performance on time to event data

6.4 Multi-label classification

The last scenario included in our study is multi-label learning. The average achieved performances are shown in Table 10, while the results of the statistical analysis are reflected in Figure 8.

For this scenario, RF achieves the highest performance followed by the LTreeX methods, whereas Small RF and Best Trees perform worse, the difference in this case is not significant though. Like in the survival and regression case, and unlike the binary classification set-up, the tree-based method performs slightly better than

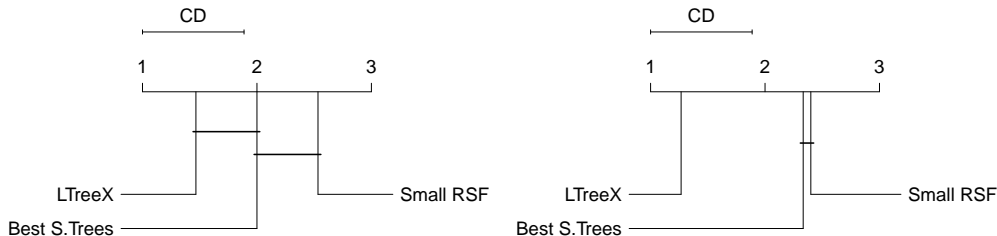


Figure 5: Friedman-Nemenyi test for dissimilarity measure (time-to-event), full tree-based representation to the left, and path-based representation to the right.

Table 10: Average achieved (weighted) AUROC across multi-label classification datasets. In bold, the best achieved performance excluding the black-box RF.

| RF | LTreeX paths | LTreeX trees | avg. nb. of paths | DT | Best Trees | Small RF |
|--------|--------------|---------------|-------------------|--------|------------|----------|
| 0.8473 | 0.7958 | 0.8032 | 3.18 | 0.7378 | 0.7647 | 0.7496 |

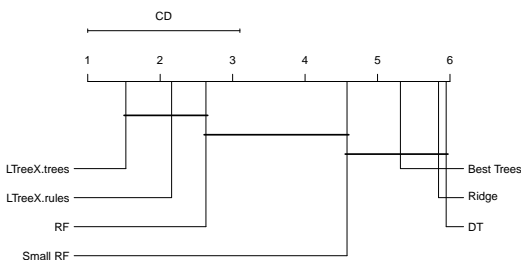


Figure 6: Friedman-Nemenyi test, results regarding performance achieved with regression tasks.

the path-based one. More details can be found in Table 16

Regarding the dissimilarity among extracted learners, the results are similar to the regression scenarios: LTreeX achieves the highest average dissimilarity within both tree and path-based approach, followed by Best Trees. Figure 9 reports the statistical results, while the dataset-specific

values are shared in Table 17.

6.5 Ablation Studies

As thoroughly described above, the LTreeX methodology consists of three main steps: 1) the pre-selection of the most relevant decision trees within the random forest, 2) the projection of the vectorization of the trees to a low-dimensional space and 3) the clustering step. The clustering part of our method is a fundamental part of our approach and it would not be possible to be removed. To this end, in this ablation study we evaluate the added value of first, the tree pre-selection mechanism and second, the dimensionality reduction step of our method.

Hence, we have performed an ablation study where each step is separately employed measuring each time the end performance of our method. More specifically, we have compared four scenarios:



Figure 7: Friedman-Nemenyi test for dissimilarity measure for the regression set-up. Full tree-based representation to the left, path-based representation to the right.

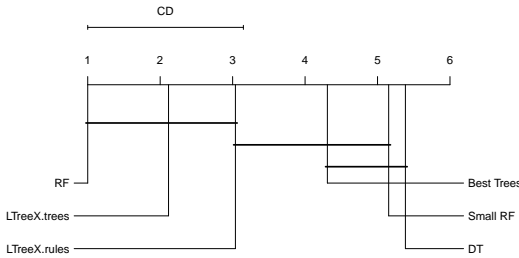


Figure 8: Friedman-Nemenyi test, results regarding performance achieved with multi-label tasks.

- We apply neither dimensionality reduction (PCA) nor tree-selection (i.e., a baseline version of our method where both steps 1 and 2 are removed);
- We only apply tree-selection (i.e., a version where only step 1 is included);
- We employ only dimensionality reduction without pre-selecting any trees from the forest (i.e., a version where only step 2 is included);
- LTreesX paths: our proposed method including all steps described above.

The results of this analysis are presented in Table 11. Here, we present the obtained results

that related to survival-analysis datasets while the results related to the other tasks are provided in the Appendix Tables 18, 19 and 20. As it is shown in the table, the best (average) performance is achieved when all steps of the proposed approach are included, affirming the added value of each step. More specifically, we can observe a substantial decrease in the average performance when we remove both steps 1 and 2. It can be also clearly noted that the use of both tree-selection as well as dimensionality reduction prior to clustering yields better results.

More specifically, some datasets benefit substantially from the inclusion of step 1 (tree-selection), as shown in “B.C. survival”, “DBCD” and “DLBCL”, where the C-index has improved by approximately 10%. Similarly, only including step 2 (that is, only PCA) often improves upon the baseline version, as exemplified in the “echocardiogram” and “ALS” datasets. Since these steps facilitate the clustering step, this improvement is expected.

Furthermore, one could notice that the difference in performance between including only step 1 and LTreesX paths is relatively small, however, in high-dimensional datasets, such as “DBCD” and “DLBCL”, a more prominent advantage is noticed. It has to be mentioned that in high dimensional datasets the application of a

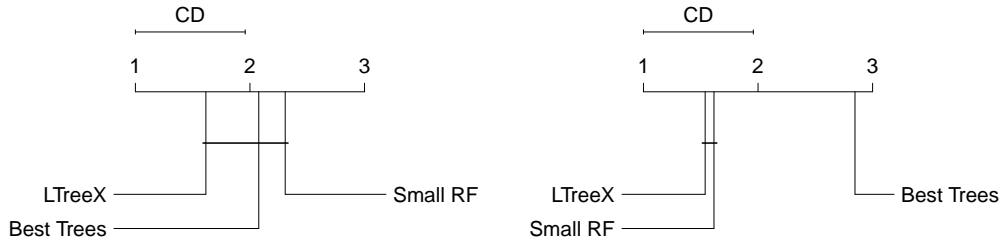


Figure 9: Friedman-Nemenyi test for dissimilarity measure on the multi-label datasets, the full tree-based representation to the left, and path-based representation to the right.

dimensionality reduction step can substantially facilitate the subsequent clustering part of our method.

6.6 Explanations with LTreeX

In this Section, we show how LTreeX works in practice. To do so, we pick one example to be explained from the “boston housing” regression data. This dataset contains 506 neighbourhoods (or “towns”), each described by 14 covariates. The predicted value is the median price value, normalised in our case to the $[0, 1]$ interval. For the first sample of the dataset, the pre-selection, vectorisation and clustering step, lead to the cluster plot shown in Figure 10.

The final extracted paths are the ones with index 44, 76 and 72, with respective weights equal to 0.28, 0.5 and 0.22. The first rulepath, representative of the dark blue cluster in 10 is shown under the block “Rulepath 44”:

Rulepath 44 predicting sample $i = 0$

If:

$$\begin{aligned} 6.543 &\leq \text{rm} \leq 6.978 \\ 5.410 &\leq \text{lstat} \leq 15.405 \\ \text{dis} &\leq 2.728 \end{aligned}$$

Then:

$$y = 0.4033$$

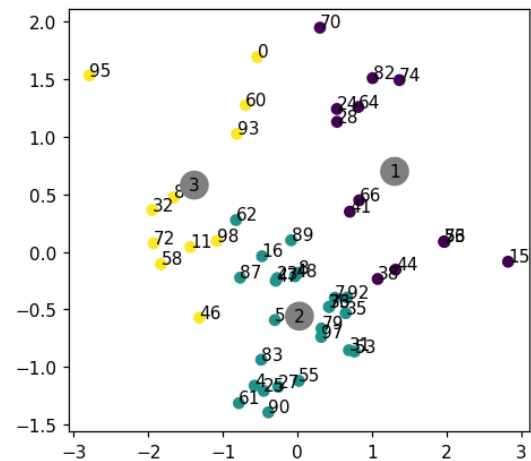


Figure 10: LTreeX performed on sample $i = 0$ in the test set, fold 1. Rules number 44, 76 and 72 are chosen in this case. The learners do not necessarily appear closest to the centre of their cluster since the first 2 principal components are plotted. Originally, the components were 14.

The features used for the splitting are `rm`, `lstat` and `dis`, which respectively indicate: the average number of rooms per dwelling, percentage of lower status population, and the weighted distances to five Boston employment centres. As of the second cluster, the representing “Rulepath 72” is shown to the end-user.

Table 11: Ablation study results on the time-to-event datasets. In bold, the best achieved performance excluding the black-box RSF.

| Time-to-event data | No PCA nor tree-selection | Only tree-selection | Only PCA | LTreesX paths |
|--------------------|---------------------------|---------------------|---------------|---------------|
| addicts | 0.6518 | 0.6485 | 0.6535 | 0.6479 |
| ALS | 0.7739 | 0.8039 | 0.8071 | 0.8061 |
| B.C. survival | 0.6023 | 0.6922 | 0.6532 | 0.6787 |
| DBCD | 0.6135 | 0.7488 | 0.673 | 0.7614 |
| DLBCL | 0.5469 | 0.6249 | 0.6013 | 0.6314 |
| echocardiogram | 0.3883 | 0.4056 | 0.4328 | 0.4119 |
| FLChain | 0.8250 | 0.8304 | 0.828 | 0.8296 |
| gbsg2 | 0.6973 | 0.7035 | 0.6992 | 0.7032 |
| lung | 0.5944 | 0.6125 | 0.6027 | 0.6137 |
| NHANES I | 0.8174 | 0.8196 | 0.8133 | 0.8179 |
| PBC | 0.8434 | 0.8472 | 0.8444 | 0.8477 |
| rotterdam (excl.) | 0.7857 | 0.7983 | 0.7925 | 0.7988 |
| rotterdam (incl.) | 0.8988 | 0.9047 | 0.9027 | 0.9045 |
| veteran | 0.7406 | 0.7323 | 0.7406 | 0.7320 |
| whas500 | 0.7413 | 0.7441 | 0.7433 | 0.7446 |
| avg. perform | 0.7014 | 0.7278 | 0.7192 | 0.7286 |

Rulepath 72 predicting sample $i = 0$

If:

$$\begin{aligned} \text{lstat} &\leq 9.715 \\ 6.728 &\leq \text{rm} \leq 7.445 \\ \text{pratio} &\geq 18.9 \\ \text{age} &\leq 80.3 \end{aligned}$$

Then:

$$y = 0.4044$$

Rulepath 76 predicting sample $i = 0$

If:

$$\begin{aligned} 6.542 &\leq \text{rm} \leq 6.92 \\ 4.915 &\leq \text{lstat} \leq 16.215 \\ \text{dis} &\leq 3.939 \\ \text{ID} &\geq 287 \end{aligned}$$

Then:

$$y = 0.4314$$

We can see that some of the splitting covariates of this rulepath are unseen, with **pratio** (pupil-teacher ratio in town) and **age** (related to the age of the buildings in the neighbourhood) replacing **dis**. Finally, we analyse the third rulepath:

This rulepath differs from the previous one in splitting along the **ID** covariate, an indication of the index of the sample in the original dataset. Other covariates, namely **rm** and **lstat**, appear in all three selected rulepaths, suggesting that these are important predictors for this sample.

To get the final prediction of LTreeX, the weighted combination of the three paths following Equation 3 is computed, leading to a prediction of $\bar{y} = 0.4101$, very close to RF’s $\hat{y} = 0.4102$ and to the true value $y = 0.3867$.

7 Conclusion and future work

In this article, we proposed a novel methodology that interprets random forests by extracting a surrogate model consisting of the most representative decision trees in the forest. Our proposed method, LTreeX, is evaluated using 71 real world datasets, which belong to four different predictive tasks, namely binary classification, time-to-event prediction, multi-label classification, and regression.

LTreeX achieves high levels of predictive performance by extracting a small number of learners, which we limited to four in our experiments. Its performance is often on par with that of random forests, and even outperforms this benchmark in regression tasks. Even in the least favourable case, namely multi-label classification, LTreeX is not significantly outperformed by random forests. We can therefore conclude that our method achieves its intended goal of explaining the prediction of a random forest with a few rules, without giving up on predictive performance.

When a comparison is drawn against other methods that extract a similar number of trees from a random forest, LTreeX outperforms them in all analysed scenarios, and the difference is statistically significant in nearly all cases. LTreeX also statistically significantly outperforms C443, a recent method from the literature, and single decision trees. Furthermore, when compared against ante-hoc explainable methods

that do not rely on a tree structure, such as logistic regression, Cox-PH and Ridge regression, LTreeX comes on top. A detailed comparison also shows that linear models can be more effective than tree-based ones in a few tasks, suggesting that these two families can effectively complement each other. This trend is most visible in the binary classification set-up.

We also studied the dissimilarity of the trees (or paths) extracted by LTreeX. We showed that LTreeX has a greater dissimilarity compared to picking the same number of random trees from the ensemble, or picking the same number of best performing trees. In four of the eight analysed cases, this difference in dissimilarity is statistically significant. This dissimilarity in LTreeX is enforced during the clustering step, and it is remarkable that it proves to be successful despite the fact the the optimal number of clusters K is not optimised for dissimilarity, but rather for faithfulness to the original random forest. Finally, the high average dissimilarity guarantees that the final extracted trees or rules are not redundant, and they give diverse possible explanations to the end user.

Although in this paper we focus on the random forest ensemble model, our proposed approach is robust and has been designed in a way that is able to accommodate other tree-ensemble models such as Bagging or Extremely Randomized Trees. We also designed LTreeX so that it can handle other variations of random forests such as Survival Random Forest and Random Forest Regression. To our knowledge, no other related work is as versatile as LTreeX in providing explanations in so many different scenarios, or at least, no such experimental results have been reported.

Our method also has some limitations, which are similar to other methods that extract learn-

ers from a tree ensemble. Firstly, the interpretability of the resulting rules is challenged when the features themselves are not interpretable. Another possible limitation to the interpretability of LTreeX paths arises when the trees of the ensemble model are too large. To tackle this limitation, we advise the end-user to set more stringent stopping criteria (increasing the minimum number of samples per leaf, or setting a limit to the tree depth). In case of performance loss of the resulting RF, the number of original learners can be increased.

Directions for future work include exploring new tree representation approaches, tailoring them to the data at hand or to the end user, and evaluating LTreeX on an even broader set of tasks, such as multi-target regression, time-series prediction or online learning. marks from the AI-ML-AI and the PharML reviewers

Appendix A

Here we include the results of the performance and dissimilarity results as well as the ablation studies of the remaining scenarios.

Table 12: Average predictive performance (C-index) across time-to-event datasets. Our proposed methods is shown in under the name “LTreeX” in its two configurations: tree and path-based.

| | RSF | LTreeX paths | LTreeX trees | Best Trees | Small RSF | Single SDT | Regul. Cox-PH | average nb. paths |
|-------------------|--------|-----------------|-----------------|------------|---------------|------------|------------------|----------------------|
| addicts | 0.6478 | 0.6479 | 0.6488 | 0.6206 | 0.6334 | 0.6425 | 0.6563 | 2.88 |
| ALS* | 0.8062 | 0.8061 | 0.8062 | 0.7623 | 0.7133 | 0.6925 | 0.7814 | 2.94 |
| B.C. survival | 0.6863 | 0.6787 | 0.6791 | 0.6377 | 0.5490 | 0.5150 | 0.5708 | 2.91 |
| DBCID | 0.7629 | 0.7614 | 0.7598 | 0.6150 | 0.6884 | 0.6127 | 0.7235 | 2.90 |
| DLBCL | 0.6334 | 0.6314 | 0.6312 | 0.5701 | 0.5810 | 0.5801 | 0.6129 | 2.97 |
| echocardiogram | 0.4070 | 0.4119 | 0.4101 | 0.4629 | 0.4715 | 0.4484 | 0.4096 | 2.92 |
| FLChain | 0.8307 | 0.8296 | 0.8317 | 0.8148 | 0.8135 | 0.7712 | 0.8218 | 2.93 |
| gbsg2 | 0.7033 | 0.7032 | 0.7035 | 0.6640 | 0.6719 | 0.6330 | 0.6876 | 2.93 |
| lung | 0.6139 | 0.6137 | 0.6148 | 0.5682 | 0.5742 | 0.5845 | 0.6056 | 2.88 |
| NHANES I* | 0.8181 | 0.8179 | 0.8190 | 0.7811 | 0.7691 | 0.7424 | 0.8043 | 2.78 |
| PBC | 0.8477 | 0.8477 | 0.8486 | 0.7891 | 0.7950 | 0.7669 | 0.8192 | 2.91 |
| rotterdam (excl.) | 0.7985 | 0.7988 | 0.7990 | 0.7646 | 0.7739 | 0.7462 | 0.7668 | 2.85 |
| rotterdam (incl.) | 0.9045 | 0.9045 | 0.9044 | 0.8760 | 0.8523 | 0.8314 | 0.8996 | 2.94 |
| veteran | 0.7314 | 0.7320 | 0.7314 | 0.6701 | 0.7115 | 0.7132 | 0.7452 | 2.85 |
| whas500 | 0.7455 | 0.7446 | 0.7451 | 0.6921 | 0.7330 | 0.6513 | 0.7332 | 2.93 |
| average | 0.7291 | 0.7286 | 0.7288 | 0.6859 | 0.6887 | 0.6621 | 0.7092 | 2.90 |

Table 13: Dissimilarities for time-to event data

| | LTreeX trees | Small RF trees | Best Trees trees | LTreeX paths | mini RF paths | Best Trees paths |
|-------------------|------------------------|-------------------|---------------------|------------------------|------------------|---------------------|
| addicts | 0.3227 | 0.2682 | 0.3887 | 0.3527 | 0.2692 | 0.3330 |
| ALS | 0.3720 | 0.3759 | 0.3854 | 0.8901 | 0.8782 | 0.8697 |
| B.C. survival | 0.9470 | 0.9218 | 0.9157 | 0.9765 | 0.9514 | 0.9510 |
| DBCDD | 0.9981 | 0.9975 | 0.9992 | 0.9979 | 0.9976 | 0.9990 |
| DLBCL | 0.9992 | 0.9978 | 1.0000 | 0.9983 | 0.9986 | 1.0000 |
| echocardiogram | 0.6200 | 0.6029 | 0.5380 | 0.8169 | 0.7781 | 0.7524 |
| FLChain | 0.1378 | 0.1297 | 0.1263 | 0.5114 | 0.5090 | 0.4820 |
| gbsg2 | 0.3050 | 0.2952 | 0.2626 | 0.6408 | 0.6234 | 0.6468 |
| lung | 0.4792 | 0.4700 | 0.4733 | 0.7593 | 0.7280 | 0.6955 |
| NHANES I | 0.1678 | 0.1677 | 0.1560 | 0.6718 | 0.6566 | 0.6672 |
| PBC | 0.5552 | 0.5500 | 0.5435 | 0.8174 | 0.7887 | 0.7874 |
| rotterdam (excl.) | 0.2194 | 0.2149 | 0.2186 | 0.5772 | 0.5670 | 0.5687 |
| rotterdam (incl.) | 0.2147 | 0.2102 | 0.2143 | 0.6225 | 0.6114 | 0.6097 |
| veteran | 0.5601 | 0.5336 | 0.5693 | 0.7731 | 0.7218 | 0.6916 |
| whas500 | 0.4397 | 0.4347 | 0.4447 | 0.7385 | 0.7268 | 0.7377 |
| Average | 0.4892 | 0.4780 | 0.4824 | 0.7430 | 0.7204 | 0.7194 |

Table 14: Average predictive performance (AUROC) across regress datasets. Our proposed methods is shown in under the name “LTreeX” in its two configurations: tree and path-based.

| | RF | LTreeX paths | LTreeX trees | Best Trees | Small RF | Single RDT | Regul. Ridge | average nb. paths |
|----------------------|---------------|----------------|----------------|------------|----------|------------|---------------|-------------------|
| airfoil | 3.7293 | 3.7345 | 3.7270 | 4.9578 | 5.4577 | 6.4533 | 10.6923 | 2.86 |
| AmesHousing | 2.2942 | 2.2956 | 2.2887 | 2.7922 | 2.8171 | 3.0803 | 2.2596 | 2.97 |
| auto mpg | 5.2449 | 5.2479 | 5.2322 | 6.0404 | 6.3657 | 6.4398 | 6.7639 | 2.87 |
| bike sharing | 4.8143 | 4.8048 | 4.8161 | 6.1121 | 5.7195 | 6.3458 | 7.8310 | 2.93 |
| Boston housing | 5.7692 | 5.7158 | 5.7014 | 6.8822 | 6.4897 | 7.4729 | 8.2441 | 2.88 |
| California housing | 6.1437 | 6.1466 | 6.1418 | 7.5200 | 7.1338 | 8.4651 | 10.4038 | 2.91 |
| car imports 1985 | 3.6188 | 3.6299 | 3.6119 | 4.8126 | 3.7776 | 4.5638 | 3.8388 | 2.86 |
| Computer hardware | 2.9124 | 2.9113 | 2.9282 | 4.2593 | 3.1680 | 4.2342 | 3.5394 | 2.96 |
| concrete compressive | 3.9725 | 3.9636 | 3.9706 | 5.4541 | 5.2275 | 6.0179 | 10.5303 | 2.88 |
| concrete slump | 7.3522 | 7.3277 | 7.3274 | 10.7188 | 7.6410 | 8.5191 | 9.0328 | 2.68 |
| ENB2012 cooling | 3.3860 | 3.3780 | 3.3763 | 3.8265 | 3.4837 | 3.8572 | 7.2399 | 2.89 |
| ENB2012 heating | 1.1213 | 1.1123 | 1.1129 | 1.4861 | 1.2284 | 1.3200 | 6.4403 | 2.94 |
| forest fires | 30.3814 | 30.3096 | 30.2955 | 32.3181 | 31.7221 | 32.5593 | 31.9047 | 2.91 |
| PRSA data | 3.5816 | 3.5833 | 3.5713 | 4.5521 | 4.8421 | 4.9130 | 8.8175 | 2.99 |
| slump | 6.8175 | 6.8433 | 6.8147 | 10.7731 | 8.6215 | 7.9739 | 5.0633 | 2.94 |
| students final math | 15.5578 | 15.4533 | 15.4891 | 17.8972 | 17.9734 | 18.5077 | 17.6423 | 2.80 |
| wine quality all | 7.3911 | 7.1085 | 7.1217 | 8.9961 | 8.5103 | 8.9773 | 9.3042 | 2.42 |
| wine quality red | 8.3734 | 8.0833 | 8.0493 | 9.5496 | 10.0814 | 10.1458 | 10.2919 | 2.41 |
| wine quality white | 6.4398 | 6.1950 | 6.1572 | 7.6738 | 8.2313 | 8.4254 | 9.2312 | 2.37 |
| average | 6.7843 | 6.7286 | 6.7228 | 8.2433 | 7.8153 | 8.3301 | 9.4248 | 2.81 |

Table 15: Average dissimilarity for regression datasets

| | LTreeX | | Small RF | | Best Trees | | LTreeX | | mini RF | | Best Trees | |
|----------------------|---------------|---------------|---------------|---------------|---------------|---------------|--------|-------|---------|-------|------------|-------|
| | trees | trees | trees | trees | trees | trees | paths | paths | paths | paths | paths | paths |
| airfoil | 0.1138 | 0.1084 | 0.1131 | 0.3464 | 0.3257 | 0.3448 | | | | | | |
| Ames Housing | 0.3411 | 0.3447 | 0.3421 | 0.7020 | 0.6966 | 0.7131 | | | | | | |
| auto mpg | 0.2312 | 0.2120 | 0.2325 | 0.5455 | 0.5187 | 0.5504 | | | | | | |
| bike sharing | 0.2108 | 0.2072 | 0.2179 | 0.5257 | 0.5162 | 0.5307 | | | | | | |
| Boston housing | 0.2941 | 0.2899 | 0.2980 | 0.5883 | 0.5782 | 0.5806 | | | | | | |
| California housing | 0.0434 | 0.0412 | 0.0376 | 0.4198 | 0.4067 | 0.3980 | | | | | | |
| car imports 1985* | 0.5471 | 0.5419 | 0.5357 | 0.6865 | 0.6649 | 0.7349 | | | | | | |
| Computer hardware | 0.2780 | 0.2693 | 0.2406 | 0.5096 | 0.5084 | 0.4900 | | | | | | |
| concrete compressive | 0.1626 | 0.1597 | 0.1466 | 0.4891 | 0.4674 | 0.4765 | | | | | | |
| concrete slump | 0.4812 | 0.4705 | 0.4775 | 0.6173 | 0.5697 | 0.6467 | | | | | | |
| ENB2012 cooling | 0.1417 | 0.1396 | 0.1574 | 0.5120 | 0.4989 | 0.4916 | | | | | | |
| ENB2012 heating | 0.1435 | 0.1324 | 0.1499 | 0.5041 | 0.4775 | 0.5262 | | | | | | |
| forest fires | 0.3074 | 0.2971 | 0.3176 | 0.6914 | 0.6796 | 0.6945 | | | | | | |
| PRSA | 0.0355 | 0.0340 | 0.0266 | 0.4200 | 0.4098 | 0.3986 | | | | | | |
| slump | 0.4776 | 0.4626 | 0.4701 | 0.6146 | 0.5782 | 0.6890 | | | | | | |
| students final math | 0.4938 | 0.4991 | 0.5324 | 0.7796 | 0.7555 | 0.7634 | | | | | | |
| wine quality all | 0.0995 | 0.0983 | 0.1112 | 0.5386 | 0.5407 | 0.5379 | | | | | | |
| wine quality red | 0.1897 | 0.1887 | 0.1773 | 0.5902 | 0.5828 | 0.5858 | | | | | | |
| wine quality white | 0.1133 | 0.1086 | 0.1176 | 0.5511 | 0.5325 | 0.5256 | | | | | | |
| Average | 0.2476 | 0.2424 | 0.2475 | 0.5596 | 0.5425 | 0.5620 | | | | | | |

Table 16: Average predictive performance (AUROC) across multi-label datasets. Our proposed methods is shown in under the name “LTreeX” in its two configurations: tree and path-based.

| | RF | LTreeX paths | LTreeX trees | Best Trees | Small RF | Single DT | average nb. paths |
|---------------|--------|-----------------|-----------------|------------|----------|-----------|----------------------|
| birds | 0.9199 | 0.8414 | 0.8568 | 0.7310 | 0.8054 | 0.7371 | 2.58 |
| CAL500 | 0.5781 | 0.5448 | 0.5501 | 0.5444 | 0.5355 | 0.5206 | 3.88 |
| emotions | 0.8521 | 0.8242 | 0.8323 | 0.7930 | 0.7756 | 0.7453 | 3.31 |
| enron | 0.8192 | 0.7646 | 0.7750 | 0.7263 | 0.7456 | 0.7190 | 3.57 |
| flags | 0.7458 | 0.7422 | 0.7383 | 0.6565 | 0.6835 | 0.6799 | 3.50 |
| genbase | 1.0000 | 0.9977 | 0.9977 | 0.9704 | 0.9914 | 0.9971 | 1.35 |
| langlog | 0.7575 | 0.6060 | 0.6291 | 0.5648 | 0.6201 | 0.6107 | 3.29 |
| medical | 0.9841 | 0.9556 | 0.9626 | 0.9141 | 0.9281 | 0.9279 | 3.33 |
| ng20 | 0.9631 | 0.9249 | 0.9264 | 0.8915 | 0.8747 | 0.8360 | 3.30 |
| scene | 0.9477 | 0.9226 | 0.9270 | 0.8540 | 0.8604 | 0.7865 | 2.93 |
| slashdot | 0.8691 | 0.8270 | 0.8386 | 0.7681 | 0.7745 | 0.7716 | 3.28 |
| stackex chess | 0.8330 | 0.7003 | 0.7123 | 0.6923 | 0.6802 | 0.6538 | 3.58 |
| yeast | 0.7455 | 0.6948 | 0.6959 | 0.6387 | 0.6662 | 0.6063 | 3.48 |
| average | 0.8473 | 0.7958 | 0.8032 | 0.7496 | 0.7647 | 0.7378 | 3.18 |

Table 17: Average dissimilarity of multi-label data.

| | LTreeX trees | Small RF trees | Best Trees trees | LTreeX paths | mini RF paths | Best Trees paths |
|---------------|------------------------|-------------------|---------------------|------------------------|------------------|---------------------|
| birds | 0.7866 | 0.7852 | 0.7904 | 0.9667 | 0.9636 | 0.9587 |
| CAL500 | 0.5952 | 0.5934 | 0.5951 | 0.9302 | 0.9264 | 0.9257 |
| emotions | 0.6022 | 0.5996 | 0.5957 | 0.9432 | 0.9255 | 0.9197 |
| enron | 0.7241 | 0.7237 | 0.7209 | 0.9667 | 0.9685 | 0.9666 |
| flags | 0.4731 | 0.4669 | 0.4970 | 0.8170 | 0.7819 | 0.7723 |
| genbase | 0.6095 | 0.6127 | 0.5722 | 0.9015 | 0.8970 | 0.8863 |
| langlog | 0.8133 | 0.8110 | 0.8122 | 0.9789 | 0.9781 | 0.9717 |
| medical | 0.7393 | 0.7380 | 0.7452 | 0.9339 | 0.9366 | 0.9319 |
| ng20 | 0.6138 | 0.6125 | 0.6199 | 0.8946 | 0.9031 | 0.8830 |
| scene | 0.6851 | 0.6843 | 0.6886 | 0.9749 | 0.9683 | 0.9639 |
| slashdot | 0.5839 | 0.5837 | 0.5809 | 0.8590 | 0.8711 | 0.8602 |
| stackex chess | 0.6247 | 0.6248 | 0.6158 | 0.9062 | 0.9183 | 0.9128 |
| yeast | 0.3829 | 0.3844 | 0.3780 | 0.9302 | 0.9237 | 0.9110 |
| Average | 0.6334 | 0.6323 | 0.6317 | 0.9233 | 0.9202 | 0.9126 |

Table 18: Ablation study results on the multi-label classification datasets. In bold, the best achieved performance.

| Multi-label | No PCA nor tree-selection | Only Tree-selection | Only PCA |
|---------------|------------------------------|------------------------|---------------|
| CAL500 | 0.5197 | 0.5476 | 0.5362 |
| birds | 0.7821 | 0.8329 | 0.8198 |
| emotions | 0.7532 | 0.8302 | 0.7998 |
| enron | 0.6976 | 0.7683 | 0.7343 |
| flags | 0.6985 | 0.7422 | 0.7159 |
| genbase | 0.9984 | 0.9977 | 0.9992 |
| langlog | 0.587 | 0.5901 | 0.5802 |
| medical | 0.8997 | 0.9527 | 0.9262 |
| ng20 | 0.8707 | 0.9252 | 0.9035 |
| scene | 0.8124 | 0.9204 | 0.9092 |
| slashdot | 0.7892 | 0.826 | 0.8085 |
| stackex_chess | 0.6534 | 0.6944 | 0.6748 |
| yeast | 0.6102 | 0.7028 | 0.6542 |
| avg. perform | 0.744 | 0.7947 | 0.774 |

Table 19: Ablation study results on the binary classification datasets. In bold, the best achieved performance.

| Binary classification | No PCA nor tree-selection | Only Tree-selection | Only PCA |
|---------------------------|---------------------------|---------------------|---------------|
| blood | 0.6992 | 0.7038 | 0.7017 |
| breast_cancer_diagnostic | 0.9838 | 0.9868 | 0.9836 |
| breast_cancer_original | 1.0 | 1.0 | 1.0 |
| breast_cancer_prognostic | 0.4641 | 0.5278 | 0.5267 |
| breast_cancer_coimba | 0.7385 | 0.7569 | 0.7354 |
| Colonoscopy-green | 0.9 | 0.8859 | 0.9333 |
| Colonoscopy_hinselmann | 0.65 | 0.5708 | 0.6167 |
| Colonoscopy_schiller | 0.5954 | 0.5846 | 0.6015 |
| divorce | 0.9516 | 0.9471 | 0.9758 |
| Flowmeters | 0.9457 | 0.9971 | 0.9629 |
| haberman | 0.6604 | 0.6847 | 0.6836 |
| hcc-survival | 0.7731 | 0.8231 | 0.7931 |
| ionosphere | 0.9518 | 0.976 | 0.974 |
| LSVT_voice_rehabilitation | 0.8471 | 0.8544 | 0.8471 |
| mamographic | 0.8428 | 0.849 | 0.8504 |
| musk | 0.8426 | 0.9422 | 0.936 |
| parkinson | 0.8587 | 0.901 | 0.9142 |
| risk_factors | 0.9339 | 0.9355 | 0.9321 |
| simulation_crashes | 0.9143 | 0.903 | 0.9137 |
| sonar | 0.8711 | 0.9151 | 0.9211 |
| SPECT | 0.7848 | 0.7537 | 0.7708 |
| SPECTF | 0.7331 | 0.8009 | 0.7881 |
| vertebral_column_data | 0.9443 | 0.9514 | 0.9458 |
| wholesale | 0.9511 | 0.9522 | 0.9515 |
| avg. perform | 0.8266 | 0.8418 | 0.8441 |

Table 20: Ablation study results on the regression datasets. In bold, the best achieved performance.

| Regression | No PCA nor tree-selection | Only Tree-selection | Only PCA |
|-------------------------------|---------------------------|---------------------|--------------|
| airfoil | 3.94 | 3.75 | 3.81 |
| AmesHousing | 2.81 | 2.29 | 6.21 |
| auto_mpg | 5.43 | 5.24 | 8.17 |
| bike_sharing | 4.97 | 4.81 | 3.63 |
| boston_housing | 5.79 | 5.72 | 6.28 |
| california_housing | 6.28 | 6.14 | 7.24 |
| car_imports_1985_imputed | 3.73 | 3.6 | 3.15 |
| Computer_hardware | 2.86 | 2.92 | 2.89 |
| concrete_compressive_strength | 4.01 | 3.95 | 3.40 |
| concrete_slump_data | 7.72 | 7.32 | 3.76 |
| ENB2012_cooling | 3.36 | 3.37 | 6.71 |
| ENB2012_heating | 1.13 | 1.11 | 4.09 |
| forest_fires | 30.06 | 30.24 | 15.89 |
| PRSA_data | 3.68 | 3.57 | 2.31 |
| slump_dataset | 6.53 | 6.88 | 7.24 |
| students_final_math | 16.47 | 15.51 | 1.12 |
| wine_quality_all | 7.3 | 7.04 | 5.82 |
| wine_quality_red | 8.03 | 7.89 | 5.22 |
| wine_quality_white | 6.31 | 6.04 | 4.86 |
| avg. perform | 6.9 | 6.7 | 6.78 |

Declarations

Funding: This research received funding from the Flemish Government (AI Research Program) and the Research Fund Flanders (project G080118N and G0A2120N).

Conflicts of interest: None

Consent to participate: NA

Consent for publication: We give our consent for the publication of identifiable elements of this paper, given appropriate referencing.

Code, data and material availability: The code as well as the dataset used to replicate the obtained results will be available on GitHub upon acceptance.

Ethics approval: NA

Authors' contributions: Conceptualisation of the idea: KD, FKN, KP, CV; algorithm implementation: KD, FKN; original draft manuscript preparation: KD; reviewing and editing of the manuscript: FKN, KP, CV; project supervision: CV.

References

- [1] Christine M. Cutillo et al. *Machine intelligence in healthcare—perspectives on trustworthiness, explainability, usability, and transparency*. Dec. 2020. DOI: [10.1038/s41746-020-0254-2](https://doi.org/10.1038/s41746-020-0254-2). URL: <https://doi.org/10.1038/s41746-020-0254-2>.
- [2] Mary T. Dzindolet et al. “The role of trust in automation reliance”. In: *International Journal of Human-Computer Studies* 58.6 (June 2003), pp. 697–718. ISSN: 10715819. DOI: [10.1016/S1071-5819\(03\)00038-7](https://doi.org/10.1016/S1071-5819(03)00038-7). URL: <https://linkinghub.elsevier.com/retrieve/pii/S1071581903000387>.
- [3] Christoph Molnar, Giuseppe Casalicchio, and Bernd Bischl. “Interpretable Machine Learning – A Brief History, State-of-the-Art and Challenges”. In: *Communications in Computer and Information Science* 1323.01 (2020), pp. 417–431. ISSN: 18650937. DOI: [10.1007/978-3-030-65965-3_28](https://doi.org/10.1007/978-3-030-65965-3_28). arXiv: [2010.09337](https://arxiv.org/abs/2010.09337).
- [4] Jerome H. Friedman. “Greedy function approximation: A gradient boosting machine”. In: *Annals of Statistics* 29.5 (2001), pp. 1189–1232. ISSN: 00905364. DOI: [10.1214/aos/1013203451](https://doi.org/10.1214/aos/1013203451). URL: https://www.jstor.org/stable/2699986?casa_token=kc-IzB-MUDsAAAAA:JAC8GrBaceml6rGLzj_NG87MSpKtSrE2To6jWb2gtQ-AaURB5x-VzkPoSiFDXmyQYiokjoH5KG140004uC2Lcw1JsDRGm_25dzZXF7oH8tLRwsjAko.
- [5] Alex Goldstein et al. “Peeking Inside the Black Box: Visualizing Statistical Learning With Plots of Individual Conditional Expectation”. In: *Journal of Computational and Graphical Statistics* 24.1 (2015), pp. 44–65. ISSN: 15372715. DOI: [10.1080/10618600.2014.907095](https://doi.org/10.1080/10618600.2014.907095). arXiv: [1309.6392](https://arxiv.org/abs/1309.6392).

- [6] Marco Tulio Ribeiro, Sameer Singh, and Carlos Guestrin. “Why should i trust you?” Explaining the predictions of any classifier”. In: *Proceedings of the ACM SIGKDD International Conference on Knowledge Discovery and Data Mining* 13-17-Aug (2016), pp. 1135–1144. DOI: [10.1145/2939672.2939778](https://doi.org/10.1145/2939672.2939778). eprint: [arXiv:1602.04938v3](https://arxiv.org/abs/1602.04938v3).
- [7] Scott M. Lundberg and Su In Lee. “A unified approach to interpreting model predictions”. In: *Advances in Neural Information Processing Systems* 2017-Decem.Section 2 (2017), pp. 4766–4775. ISSN: 10495258. arXiv: [1705.07874](https://arxiv.org/abs/1705.07874).
- [8] Leo Breiman. “Random forests”. In: *Machine Learning* 45.1 (Oct. 2001), pp. 5–32. ISSN: 08856125. DOI: [10.1023/A:1010933404324](https://doi.org/10.1023/A:1010933404324). URL: <https://link.springer.com/article/10.1023/A:1010933404324>.
- [9] Klest Dedja et al. “Explaining a Random Survival Forest by extracting prototype rules”. In: *ECML-PKDD , PharML Workshop, Bilbao, Spain (online)*. Springer, *PharML Workshop, Bilbao, Spain (online)*. Springer (2021), pp. 1–8.
- [10] Hugh A Chipman, Edward I George, and Robert E Mcculloch. “Making sense of a Forest of trees”. In: July (1998).
- [11] A Mead. “Review of the Development of Multidimensional Scaling Methods”. In: *Journal of the Royal Statistical Society. Series D (The Statistician)* 41.1 (1992), pp. 27–39.
- [12] Xun Zhao et al. “IForest: Interpreting Random Forests via Visual Analytics”. In: *IEEE Transactions on Visualization and Computer Graphics* 25.1 (2019), pp. 407–416. ISSN: 19410506. DOI: [10.1109/TVCG.2018.2864475](https://doi.org/10.1109/TVCG.2018.2864475).
- [13] Geoffrey E Hinton and Sam Roweis. “Stochastic neighbor embedding”. In: *Advances in neural information processing systems* 15 (2002).
- [14] Yichen Zhou and Giles Hooker. “Interpreting Models via Single Tree Approximation”. In: *Cmm* (2016), pp. 1–15. arXiv: [1610.09036](https://arxiv.org/abs/1610.09036). URL: <http://arxiv.org/abs/1610.09036>.
- [15] Alexander Moore et al. “Transparent tree ensembles”. In: *41st International ACM SIGIR Conference on Research and Development in Information Retrieval, SIGIR 2018* (2018), pp. 1241–1244. DOI: [10.1145/3209978.3210151](https://doi.org/10.1145/3209978.3210151).
- [16] Satoshi Hara. “Making Tree Ensembles Interpretable : A Bayesian Model Selection Approach”. In: *International Conference on Artificial Intelligence and Statistics, AISTATS 2018* 84 (2018).
- [17] Aniek Sies and Iven Van Mechelen. “C443: a Methodology to See a Forest for the Trees”. In: *Journal of Classification* 1 (2020). ISSN: 14321343. DOI: [10.1007/s00357-019-09350-4](https://doi.org/10.1007/s00357-019-09350-4).
- [18] Dragi Kocev et al. “Tree ensembles for predicting structured outputs”. In: *Pattern Recognition* 46.3 (Mar. 2013), pp. 817–833. ISSN: 00313203. DOI: [10.1016/j.patcog.2012.09.023](https://doi.org/10.1016/j.patcog.2012.09.023).
- [19] F. Pedregosa et al. *Scikit-learn: Machine Learning in Python*. Tech. rep. 2011, pp. 2825–2830.

- [20] Celine Vens et al. “Decision trees for hierarchical multi-label classification”. In: *Machine Learning* 73.2 (Nov. 2008), pp. 185–214. ISSN: 08856125. DOI: [10.1007/s10994-008-5077-3](https://doi.org/10.1007/s10994-008-5077-3). URL: <https://link.springer.com/article/10.1007/s10994-008-5077-3>.
- [21] Ping Wang, Yan Li, and Chandan K. Reddy. “Machine learning for survival analysis: A survey”. In: *ACM Computing Surveys* 51.6 (2019), pp. 1–39. ISSN: 15577341. DOI: [10.1145/3214306](https://doi.org/10.1145/3214306). arXiv: [1708.04649](https://arxiv.org/abs/1708.04649).
- [22] Michael LeBlanc and John Crowley. “Survival trees by goodness of split”. In: *Journal of the American Statistical Association* 88.422 (1993), pp. 457–467. ISSN: 1537274X. DOI: [10.1080/01621459.1993.10476296](https://doi.org/10.1080/01621459.1993.10476296).
- [23] Leo Breiman. *Software for the masses*. 2002. URL: <http://www.stat.berkeley.edu/users/breiman>.
- [24] Hemant Ishwaran et al. “Random survival forests”. In: *Annals of Applied Statistics* 2.3 (2008), pp. 841–860. ISSN: 19326157. DOI: [10.1214/08-AOAS169](https://doi.org/10.1214/08-AOAS169). arXiv: [arXiv:0811.1645v1](https://arxiv.org/abs/0811.1645v1).
- [25] Richard Peto and Julian Peto. “Asymptotically Efficient Rank Invariant Test Procedures”. In: *Journal of the Royal Statistical Society. Series A (General)* 135.2 (1972), p. 185. ISSN: 00359238. DOI: [10.2307/2344317](https://doi.org/10.2307/2344317). URL: <https://www.jstor.org/stable/10.2307/2344317?origin=crossref>.
- [26] E. L. Kaplan and Paul Meier. “Nonparametric Estimation from Incomplete Observations”. In: *Journal of the American Statistical Association* 53.282 (1958), pp. 457–481. ISSN: 01621459. URL: <http://www.jstor.org/stable/2281868>.
- [27] Mousumi Banerjee, Ying Ding, and Anne-Michelle Noone. “Identifying representative trees from ensembles”. In: *Statistics in Medicine* 31.15 (July 2012), pp. 1601–1616. ISSN: 02776715. DOI: [10.1002/sim.4492](https://doi.org/10.1002/sim.4492). URL: <https://onlinelibrary.wiley.com/doi/10.1002/sim.4492>.
- [28] Karl Pearson. “LIII. On lines and planes of closest fit to systems of points in space”. In: *The London, Edinburgh, and Dublin Philosophical Magazine and Journal of Science* 2 (11 Nov. 1901), pp. 559–572. ISSN: 1941-5982. DOI: [10.1080/14786440109462720](https://doi.org/10.1080/14786440109462720). URL: <https://www-tandfonline-com.kuleuven.e-bronnen.be/doi/abs/10.1080/14786440109462720>.
- [29] Sergei Vassilvitskii and David Arthur. “k-means++: The advantages of careful seeding”. In: *Proceedings of the eighteenth annual ACM-SIAM symposium on Discrete algorithms*. 2006, pp. 1027–1035.
- [30] James Lepkowski et al. *A Multivariate Technique for Multiply Imputing Missing Values Using a Sequence of Regression Models*. Tech. rep. 1. 2001. URL: <https://www.researchgate.net/publication/244959137>.

- [31] Stef Van Buuren. “Multiple imputation of discrete and continuous data by fully conditional specification”. In: *Statistical Methods in Medical Research* 16.3 (June 2007), pp. 219–242. DOI: [10.1177/0962280206074463](https://doi.org/10.1177/0962280206074463). URL: www.scopus.com,.
- [32] David R Cox. “Regression models and life-tables”. In: *Journal of the Royal Statistical Society: Series B (Methodological)* 34.2 (1972), pp. 187–202.
- [33] Janez Demšar. “Statistical comparisons of classifiers over multiple data sets”. In: *Journal of Machine Learning Research* 7 (2006), pp. 1–30. ISSN: 15337928.